

## Nonlinear Terahertz Emission in Semiconductor Microcavities

I. G. Savenko,<sup>1,2</sup> I. A. Shelykh,<sup>1,3</sup> and M. A. Kaliteevski<sup>2,4</sup>

<sup>1</sup>Science Institute, University of Iceland, Dunhagi-3, IS-107, Reykjavik, Iceland

<sup>2</sup>Academic University—Nanotechnology Research and Education Centre, Khlopina 8/3, 194021, St. Petersburg, Russia

<sup>3</sup>International Institute of Physics, Avenida Odilon Gomes de Lima, 1772, Capim Macio, 59078-400, Natal, Brazil

<sup>4</sup>Ioffe Physical-Technical Institute, Polytekhnicheskaya 26, 194021, St. Petersburg, Russia

(Received 7 March 2011; revised manuscript received 28 May 2011; published 6 July 2011)

We consider the nonlinear terahertz emission by the system of cavity polaritons in the regime of polariton lasing. To account for the quantum nature of terahertz-polariton coupling, we use the Lindblad master equation approach and demonstrate that quantum microcavities reveal a rich variety of nonlinear phenomena in the terahertz range, including bistability, short terahertz pulse generation, and terahertz switching.

DOI: 10.1103/PhysRevLett.107.027401

PACS numbers: 78.67.Pt, 78.45.+h, 78.47.jm, 78.66.Fd

*Introduction.*—The terahertz (THz) band remains the last region of the electromagnetic spectrum which does not have a wide application in modern technology due to the lack of a solid state source of THz radiation which is compact, reliable, and scalable [1]. The fundamental objection preventing realization of such a source is the small rate of spontaneous emission of the THz photons. According to the Fermi golden rule, this rate is about tens of inverse milliseconds, while the lifetime of the photoexcited carrier typically lies in the picosecond range due to efficient interaction with phonons [2,3]. The spontaneous emission rate can be increased by application of the Purcell effect when the emitter of THz is placed in a cavity for the THz mode [4,5], but even in this case cryogenic temperatures are required to provide quantum efficiency of the order of about 1% for a typical quantum cascade structure.

Recently, it was proposed that the rate of spontaneous emission for THz photons can be additionally increased by bosonic stimulation if a radiative transition occurs into a condensate state [6]. One example is a transition between upper and lower polariton branches in a semiconductor microcavity in the regime polariton lasing. Unfortunately, the radiative transition accompanied by emission of a THz photon between upper and lower polariton modes is forbidden, since these states have the same parity. Nevertheless, such a transition becomes possible if the upper polariton state is mixed with an exciton state of different parity. Amplification of spontaneous emission by the Purcell effect together with bosonic stimulation increases the rate of spontaneous emission by several orders of magnitude, making it comparable with the rate of scattering with an acoustic phonon. Consequently, effective emission of THz radiation can occur [6].

It is well known that strong polariton-polariton interactions in microcavities make it possible to observe pronounced nonlinear effects for the intensities of the pump orders of magnitude smaller than in other nonlinear optical systems. Among them are polariton superfluidity [7],

bistability and multistability [8,9], soliton formation [10], and others. One can expect that polariton-polariton interactions will strongly affect the process of THz emission as well. The quasiclassical approach based on the Boltzmann equations, used in Ref. [6], cannot provide a correct account of a coherent interaction of THz photons and polaritons and cannot be used for a satisfactory description of nonlinearities in the considered system. The development of a more exact quantum formalism is thus needed. This Letter is aimed at building such a formalism, which accounts for the following physical processes: coherent polariton-THz photon interaction, polariton-polariton interaction leading to the blueshift of the polariton modes, and coupling of the polaritons with acoustic phonons. The development of such a description is timely in light of intensive studies of ultrastrong light-matter coupling [11,12], single-cycle THz generation [13,14], intersubband cavity polariton physics [14,15], and control of the phase of THz radiation in both inorganic and organic structures [16,17].

*Formalism.*—We consider a model system consisting of a lower polariton state with the energy  $\epsilon_L$ , upper hybrid state with the energy  $\epsilon_U$ , THz cavity mode with the energy  $\epsilon_T$ , and incoherent polariton reservoir coupled with upper and lower polariton states via the phonon-assisted process (see Fig. 1).

The Hamiltonian of the system written in terms of the operators of secondary quantization for upper polaritons ( $a_U, a_U^+$ ), lower polaritons ( $a_L, a_L^+$ ), THz photons ( $c, c^+$ ), reservoir states ( $a_{R\mathbf{k}}, a_{R\mathbf{k}}^+$ ), and acoustic phonons ( $b_{\mathbf{k}}, b_{\mathbf{k}}^+$ ) can be represented as a sum of four terms:

$$H = H_0 + H_{\text{pol-pol}} + H_T + H_R. \quad (1)$$

The first term

$$H_0 = \epsilon_L a_L^+ a_L + \epsilon_U a_U^+ a_U + \epsilon_T c^+ c + \sum_{\mathbf{k}} \epsilon_{\mathbf{k}} a_{R\mathbf{k}}^+ a_{R\mathbf{k}} \quad (2)$$

corresponds to the energy of uncoupled upper and lower polaritonic states, the THz mode, and the polariton reservoir.

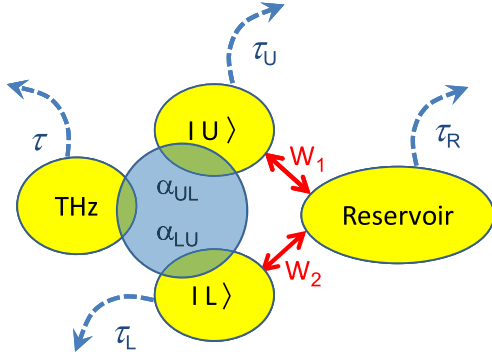


FIG. 1 (color online). The scheme of transitions in a THz emitting cavity. The upper polariton is mixed with a dark exciton state due to the application of the gate voltage  $V_g$ . The radiative transition between the upper hybrid state  $|U\rangle$  and lower polariton state  $|L\rangle$  thus becomes possible. Upper hybrid and lower polariton states are also coupled with an incoherent reservoir of the polaritons via the phonon-assisted process.

The second term

$$H_{\text{pol-pol}} = U_{LL}a_L^+a_L^-a_La_L + U_{UU}a_U^+a_U^-a_Ua_U \\ + 2U_{UL}a_U^+a_U^-a_L^+a_L + 2\sum_k(U_{LR}a_L^+a_L^- \\ + U_{UR}a_U^+a_U^-)a_{Rk}^+a_{Rk} \quad (3)$$

describes polariton-polariton interaction. The interaction constants can be estimated as  $U_{ij} = X_i^2X_j^2U$ , where  $X_i$  are Hopfield coefficients giving the percentage of the exciton fraction in the polariton states.  $X_U$  and  $X_L$  are determined by cavity geometry, and we took  $X_R = 1$  supposing that the reservoir is purely excitonic. The matrix element of the exciton-exciton scattering can be estimated as  $U \approx 6E_B a_B^2/S$  with  $E_B$  and  $a_B$  being the exciton binding energy and Bohr radius, respectively, and  $S$  the area of the system [18].

The third term

$$H_T = V_T(a_U^+a_Lc + a_Ua_L^+c^+) \quad (4)$$

describes a radiative THz transition between upper and lower polariton states. The matrix element of the THz emission can be estimated by using a standard formula for the coupling constant of the dipole transition with a confined electromagnetic mode:  $V_T = \omega^2 d \sqrt{\hbar n / 2\pi^3 \epsilon_0 c^3}$ , where  $d$  is the matrix element of the radiative transition and  $n$  the refractive index of the terahertz cavity (see, e.g., Ref. [19]).

Interaction between upper and lower polariton states and the incoherent reservoir is described by the fourth term:

$$H_R = H_R^+ + H_R^- = D_1 \sum_k (a_U a_{Rk}^+ b_k^+ + a_U^+ a_{Rk} b_k) \\ + D_2 \sum_k (a_L a_{Rk}^+ b_k + a_L^+ a_{Rk} b_k^+), \quad (5)$$

where  $b_k^+$  and  $b_k$  denote operators of creation and annihilation, respectively, of phonons with wave vector  $\mathbf{k}$  and  $D_1$  and  $D_2$  are the polariton-phonon interaction constants.

Keeping in mind that interactions described by  $H_0$ ,  $H_{\text{pol-pol}}$ , and  $H_T$  are of a coherent nature, while phonon-assisted interactions ( $H_R$ ) with a reservoir destroy coherences, the dynamics of the density matrix of system  $\rho$  is described by the Lindblad master equation, analogical to those obtained in Refs. [20,21] (see also [22]),

$$\frac{\partial \rho}{\partial t} = \frac{i}{\hbar} [\rho; H_0 + H_{\text{pol-pol}} + H_T] + \frac{\delta_{\Delta E}}{\hbar} \{ 2(H_R^+ \rho H_R^- \\ + H_R^- \rho H_R^+) - (H_R^+ H_R^- + H_R^- H_R^+) \rho - \rho (H_R^+ H_R^- \\ + H_R^- H_R^+) \} + \frac{1}{2\tau_L} \hat{L}_{a_L} + \frac{1}{2\tau_D} \hat{L}_{a_D} + \frac{1}{2\tau_R} \hat{L}_{a_R} \\ + \frac{1}{2\tau} \hat{L}_c + \frac{P}{2} \hat{L}_{a_U^+} + \frac{I}{2} \hat{L}_{c^+}, \quad (6)$$

where  $\hat{L}_A$  is the Lindblad operator defined by the formula  $\hat{L}_A = 2A\rho A^\dagger - A^\dagger A\rho - \rho A^\dagger A$ ,  $\tau_L$ ,  $\tau_U$ ,  $\tau_R$ , and  $\tau$  are lifetimes of lower polaritons, upper polaritons, polaritons in the reservoir, and THz photons, respectively, and  $P$  and  $I$  are the pumping intensities of the upper polariton state and terahertz mode, respectively. The delta function  $\delta_{\Delta E}$  denotes the conservation of energy in the process of phonon scattering. The first line accounts for the coherent processes in the system, the second and third lines correspond to the phonon-assisted coupling with an incoherent reservoir of the polaritons, and the last line accounts for the pump and the decay.

The equations for the populations of polariton states and terahertz photons can be obtained as

$$\partial_t n_i = \text{Tr} \left( \hat{n}_i \frac{\partial \rho}{\partial t} \right). \quad (7)$$

Using the mean field approximation, one gets the closed system of the dynamic equations for the occupancies  $n_L = \langle a_L^+ a_L \rangle$ ,  $n_U = \langle a_U^+ a_U \rangle$ ,  $n_{Rk} = \langle a_{Rk}^+ a_{Rk} \rangle$ , and  $n = \langle c^+ c \rangle$  connected by the correlators  $\alpha_{LU} = \langle a_L^+ a_U c^+ \rangle$  and  $\alpha_{UL} = \langle a_L a_U^+ c \rangle = \alpha_{LU}^*$  (see [22]):

$$\partial_t n_L = -2 \frac{V_T}{\hbar} \text{Im}(\alpha_{UL}) - \frac{n_L}{\tau_L} + W_2 \sum_k \{ (n_L + 1) n_{Rk} (n_k^{\text{ph}} + 1) \\ - n_L (n_{Rk} + 1) n_k^{\text{ph}} \}, \quad (8)$$

$$\partial_t n_U = 2 \frac{V_T}{\hbar} \text{Im}(\alpha_{UL}) - \frac{n_U}{\tau_U} + P + W_1 \sum_k \{ (n_U + 1) n_{Rk} n_k^{\text{ph}} \\ - n_U (n_{Rk} + 1) (n_k^{\text{ph}} + 1) \}, \quad (9)$$

$$\partial_t n_{Rq} = - \frac{n_{Rq}}{\tau_R} + W_1 \sum_k \{ n_U (n_{Rk} + 1) (n_k^{\text{ph}} + 1) \\ - (n_U + 1) n_{Rk} n_k^{\text{ph}} \} + W_2 \sum_k \{ n_L (n_{Rk} + 1) n_k^{\text{ph}} \\ - (n_L + 1) n_{Rk} (n_k^{\text{ph}} + 1) \}, \quad (10)$$

$$\partial_t n = -2 \frac{V_T}{\hbar} \text{Im}(\alpha_{UL}) - \frac{n}{\tau} + I, \quad (11)$$

$$\begin{aligned} \partial_t \alpha_{UL} = & \frac{i}{\hbar} (\tilde{\epsilon}_U - \tilde{\epsilon}_L - \epsilon_T) \alpha_{UL} - \frac{\alpha_{UL}}{\tau_{\text{corr}}} + i \frac{V_T}{\hbar} \{ (n_U + 1) n_L n \\ & - n_U (n_L + 1) (n + 1) \} + \left\{ W_1 \sum_{\mathbf{k}} (-n_{R\mathbf{k}} - n_{\mathbf{k}}^{\text{ph}} - 1) \right. \\ & \left. + W_2 \sum_{\mathbf{k}} (n_{R\mathbf{k}} - n_{\mathbf{k}}^{\text{ph}}) \right\} \alpha_{UL}. \end{aligned} \quad (12)$$

In the above expressions  $\tau_{\text{corr}}^{-1} = \tau_L^{-1} + \tau_U^{-1} + \tau_R^{-1} + \tau^{-1}$ ,  $V_T \approx 1 \mu\text{eV}$  is a coupling constant between polaritons and terahertz photons, and  $W_{1,2} \approx 2 \text{ ps}^{-1}$  are transition rates between the reservoir and upper or lower polariton states determined by polariton-phonon interaction constants  $W_{1,2} \sim |D_{1,2}|^2$ . Note that the characteristic time of THz photon emission is about 3 orders of magnitude smaller than the characteristic time of scattering with acoustic phonons. However, THz emission is dramatically enhanced by bosonic stimulation and becomes the dominant mechanism for sufficiently strong pumps.  $n_{\mathbf{k}}^{\text{ph}}$  gives the occupancies of the phonon mode determined by the Bose distribution function. For simplicity of the calculations in the present Letter, we consider the reservoir to consist of  $N$  identical states ( $N = 3 \times 10^5$ ). Note that if coherent interaction is switched off by equating  $d\alpha_{UL}/dt = 0$ , the system of equations we use transforms into the system of Boltzmann equations considered in Ref. [6].

The renormalized energies of the upper and lower polariton states are determined by their blueshifts arising from polariton-polariton interactions and read

$$\tilde{\epsilon}_U = \epsilon_U + 2 \left( U_{UU} n_U + U_{UL} n_L + U_{UR} \sum_{\mathbf{k}} n_{R\mathbf{k}} \right), \quad (13)$$

$$\tilde{\epsilon}_L = \epsilon_L + 2 \left( U_{LL} n_L + U_{UL} n_U + U_{LR} \sum_{\mathbf{k}} n_{R\mathbf{k}} \right). \quad (14)$$

Because of the difference of the Hopfield coefficients for the upper and lower polariton states, the difference  $\tilde{\epsilon}_U - \tilde{\epsilon}_L$  depends on the polariton concentrations and thus is determined by the intensity of the pump  $P$ . This dependence can have important consequences, allowing for the onset of bistability in the system (see below).

**Results and discussions.**—We consider a planar GaAs microcavity in a strong coupling regime with Rabi splitting  $\Omega_R$  between the upper and lower polariton modes equal to 16 meV (which corresponds to 4 THz) and embedded into a THz cavity with an eigenfrequency slightly different from  $\Omega_R$  and having a quality factor  $Q = 100$  [23,24]. Let us assume that initially the system is characterized by zero population of polaritons and THz photons. When the constant nonresonant pump of the upper polariton state is switched on, the number of THz photons  $n$  starts to increase until it reaches some equilibrium level defined by the radiative decay of polaritons and escape of THz radiation from the cavity, as shown in Fig. 2.

The equilibrium value of the THz population  $n$  as a function of pumping  $P$  demonstrates thresholdlike behavior. For high enough temperatures, below the threshold

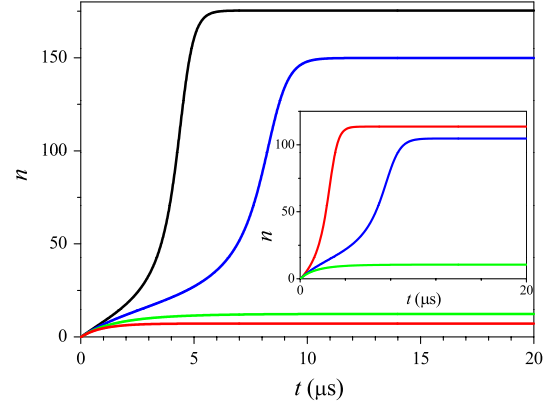


FIG. 2 (color online). Time evolution of the terahertz photon number at zero temperature for different pumps: 4500 (red line), 5000 (green line), 5500 (blue line), and 6000  $\text{ps}^{-1}$  (black line). The inset shows evolution of the THz photon number for the constant pump  $P = 6000 \text{ ps}^{-1}$  for different temperatures: 1 (red line), 10 (green line), and 20 K (blue line).

the dependence of  $n$  on  $P$  is very weak. When pumping reaches a certain threshold value, the polariton condensate is formed in the lower polariton state, radiative THz transition is amplified by bosonic stimulation, and the occupancy of the THz mode increases superlinearly together with the occupancy of lower polariton state  $n_L$  (Fig. 2, blue curve). This behavior is qualitatively the same as in the approach operating with the semiclassical Boltzmann equations. However, the decrease of temperature leads to the onset of bistability and hysteresis in the dependence  $n(P)$ . The bistable jump occurs when the intensity of the pump tunes  $\tilde{\epsilon}_U - \tilde{\epsilon}_L$  into the resonance with the cavity mode  $\epsilon_T$ . The parameters of the hysteresis loop strongly depend on the temperature (Fig. 3). It is very pronounced and broad for low temperatures, narrows with the increase of the temperature, and disappears completely at  $T \approx 20 \text{ K}$ .

The coherent nature of the interaction between excitons and THz photons makes possible the periodic exchange of energy between polaritonic and photonic modes and oscillatory dependence of the THz signal in time. Figure 3 shows

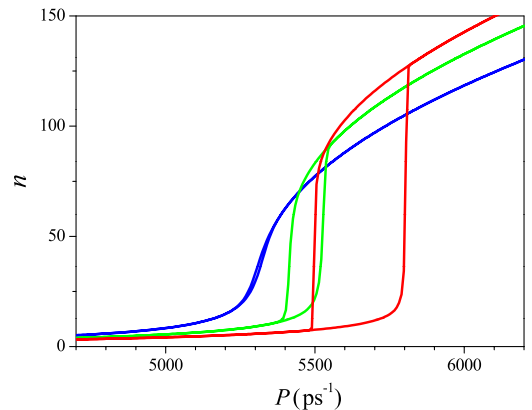


FIG. 3 (color online). Dependence of occupancy of the THz mode on the pump in the equilibrium state for different temperatures: 1 (red line), 10 (green line), and 20 K (blue line).

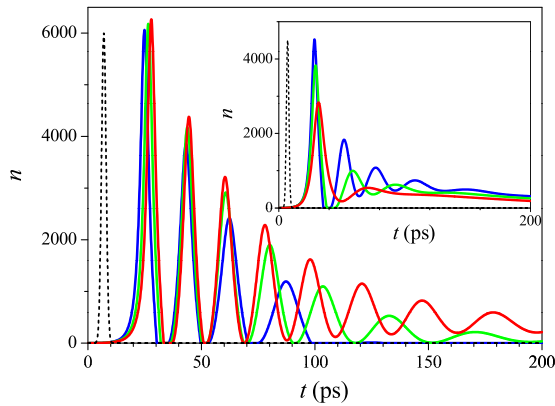


FIG. 4 (color online). The temporal dependence of the terahertz mode occupancy. The background pump is switched off; lifetimes  $\tau_L = \tau_U = 50$  ps. The temperatures are 1 (red line), 10 (green line), and 20 K (blue line). Inset:  $T = 1$  K; different lifetimes of the polariton states: 15 (red line), 20 (green line), and 25 ps (blue line).

the temporal evolution of the occupancy of the THz mode after excitation of the upper polariton state by a short pulse having a duration of about 2 ps. It is seen that the occupancy of the THz mode reveals a sequence of short pulses having a duration of dozens of picoseconds with amplitude decaying in time due to escape of THz photons from a cavity and radiative decay of polaritons. The period of the oscillations is sensitive to the number of injected polaritons  $N_0$  and decreases with increasing of  $N_0$ . If the lifetime of polaritons is less than the period of the oscillations, single pulse behavior can be observed as shown in the inset in Fig. 4. The appropriate choice of parameters can ultimately lead to a generation of THz wavelets composed of one or several THz cycles, which makes the polariton-THz system suitable for application in a short pulse THz spectroscopy.

If the system of coupled THz photons and cavity polaritons is in the state corresponding to the lower branch of the S-shaped curve in the bistability region, illumination of the system by a short THz impulse  $I(t)$  can induce its switching to the upper branch, as demonstrated in Fig. 5. One sees that the response of the system is qualitatively different for different values of the pump  $P$ . If  $P$  lies outside the bistability region, the application of a THz pulse leads to a short increase of  $n$ , but subsequently the system relaxes to its original state (red and blue curves). However, when the system is in the bistability regime, the switching occurs. Note that this effect is of a quantum nature and cannot be described by using the approach based on the semiclassical Boltzmann equations developed in Ref. [6].

**Conclusion.**—We considered the system of coupled cavity polaritons and THz photons by using the approach based on the generalized Lindblad equation for the density matrix. We showed that such a system demonstrates a variety of intriguing nonlinear effects, including bistability, THz switching, and generation of short THz wavelets.

The work was supported by Rannis “Center of excellence in polaritonics,” FP7 IRSES “POLAPHEN” and

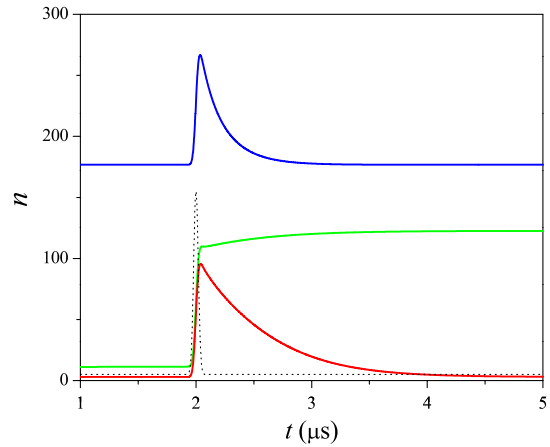


FIG. 5 (color online). System response on a short single impulse (FWHM = 40 ps, black dotted curve) for different values of the background pump: 4600 (red line), 5750 (green line), and  $6500 \text{ ps}^{-1}$  (blue line). Switching occurs only when the background pump corresponds to the bistable region (compare with Fig. 2).

“POLALAS” projects, Russian Fund of Basic Research, and COST “POLATOM” program.

- 
- [1] D. Dragoman and M. Dragoman, *Prog. Quantum Electron.* **28**, 1 (2004).
  - [2] H. T. Duc *et al.*, *Phys. Rev. B* **74**, 165328 (2006).
  - [3] T. D. Doan *et al.*, *Phys. Rev. B* **72**, 085301 (2005).
  - [4] Y. Todorov *et al.*, *Phys. Rev. Lett.* **99**, 223603 (2007).
  - [5] Y. Chassagneux *et al.*, *Nature (London)* **457**, 174 (2009).
  - [6] K. V. Kavokin *et al.*, *Appl. Phys. Lett.* **97**, 201111 (2010).
  - [7] A. Amo *et al.*, *Nature (London)* **457**, 291 (2009).
  - [8] A. Baas *et al.*, *Phys. Rev. B* **70**, 161307(R) (2004).
  - [9] N. A. Gippius *et al.*, *Phys. Rev. Lett.* **98**, 236401 (2007).
  - [10] O. A. Egorov, D. V. Skryabin, and F. Lederer, *Phys. Rev. B* **82**, 165326 (2010).
  - [11] Y. Todorov *et al.*, *Phys. Rev. Lett.* **105**, 196402 (2010).
  - [12] G. Gunter *et al.*, *Nature (London)* **458**, 178 (2009).
  - [13] F. Junginger *et al.*, *Opt. Lett.* **35**, 2645 (2010).
  - [14] Y. Todorov *et al.*, *Phys. Rev. Lett.* **102**, 186402 (2009).
  - [15] S. De Liberato and C. Ciuti, *Phys. Rev. Lett.* **102**, 136403 (2009).
  - [16] D. Oustinov *et al.*, *Nature Commun.* **1**, 69 (2010).
  - [17] M. Swoboda *et al.*, *Appl. Phys. Lett.* **89**, 121110 (2006).
  - [18] C. Ciuti *et al.*, *Phys. Rev. B* **58**, 7926 (1998).
  - [19] M. O. Scully and M. A. Zubairy, *Quantum Optics* (Cambridge University Press, Cambridge, England, 1997).
  - [20] E. B. Magnusson *et al.*, *Phys. Rev. B* **82**, 195312 (2010).
  - [21] I. G. Savenko, E. B. Magnusson, and I. A. Shelykh, *Phys. Rev. B* **83**, 165316 (2011).
  - [22] See supplemental material at <http://link.aps.org/supplemental/10.1103/PhysRevLett.107.027401> for the detailed description of the derivation of the kinetic equations.
  - [23] Y. Chassagneux *et al.*, *Nature (London)* **457**, 174 (2009).
  - [24] A. J. Gallant *et al.*, *Appl. Phys. Lett.* **91**, 161115 (2007).